

# Cloud Overlap Dependence on Atmospheric Dynamics

*C Naud*  
*Columbia University*  
*New York, New York*

*AD DelGenio*  
*National Aeronautics and Space Administration –*  
*Goddard Institute for Space Studies*  
*New York, New York*

## Introduction

Cloud parameterizations in GCMs have to make assumptions on how cloud layers are arranged with respect to each other along the vertical. These assumptions have significant impacts on the radiation budget. The commonly used assumption of random overlap for noncontiguous layers and maximum overlap for contiguous layers (Geleyn and Hollingsworth 1979) has been compared against times series of vertically pointing millimeter wave cloud radar profiles for three winter months at the United Kingdom Chilbolton site by Hogan and Illingworth (2000). They found that contiguous layers show a maximum overlap only when cloud layers are close to each other. At large separations, cloud layers showed a random overlap in accordance with Geleyn and Hollingsworth (1979). Using a similar formalism, Mace and Benson-Troth (2002; hereafter MBT02) used radar data from the four Atmospheric Radiation Measurement (ARM) Climate Research Facility (ACRF) sites over a longer period and found that contiguous layers displayed a maximum overlap for longer separations than suggested by Hogan and Illingworth (2000) at the Southern Great Plains (SGP) site. They also noticed a seasonal variation of the separations for which overlap in contiguous layers became random.

We applied the same formalism to SGP millimeter wave cloud radar data for the period where rapid update cycle (RUC)-2 data were available to relate the transition between maximum and random overlap in contiguous layers to the atmospheric dynamics.

## Method of Hogan and Illingworth (2000)

Hogan and Illingworth (2000; hereafter HI00) first derive a cloud mask from their radar reflectivity profiles and define a layer as a box 360 m high and 1-hour wide. They tested other vertical and horizontal dimensions but here we only used these. Each layer obtained as in Figure 1 will have a cloud

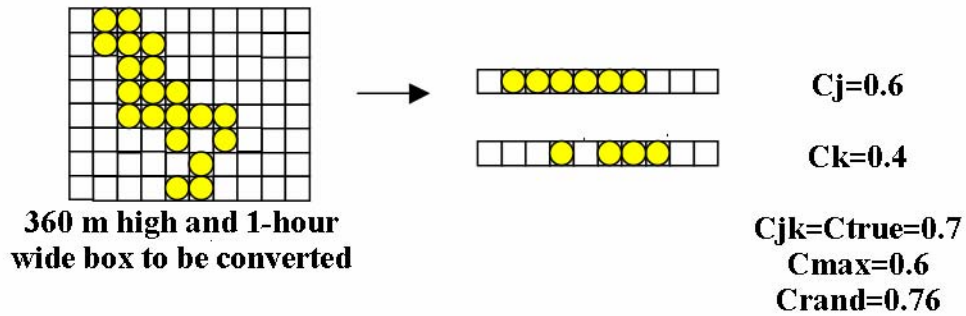


**Figure 1.** Schematic of the transformation of the radar cloud mask into 360 m and 1-hour layers (e.g., box in top layer on the right,  $C_j$ ) and how two layers give different combined cloud fractions depending on whether maximum or random overlap is assumed. In this case, the true cloud fraction is closer to the random cloud fraction.

fraction that corresponds to the number of time steps during the hour where a cloud was detected along the 360-m vertical path of the radar profile for this layer. Starting from the bottom of the atmosphere, they sort the 1-hour layers into two different sets: layers that are part of the same continuously cloudy segment of the column and layers that are separated by clear layers (cloud fraction = 0). In each subset, the cloud fractions of two layers for any possible pair are calculated ( $C_j$  and  $C_k$ ) as well as the cloud fraction of the combination of the two cloud layers ( $C_{true}$ ). In addition, the cloud fraction of the pair is evaluated assuming that the overlap is maximum ( $C_{max} = \max(C_j, C_k)$ ) or random ( $C_{rand} = C_j + C_k - C_j C_k$ ). Figure 1 shows an example with the corresponding cloud fractions.

They introduced a parameter  $\alpha$  that would be zero if the overlap is random and 1 if the overlap is maximum and related the three cloud fractions in the following manner:

$$C_{true} = \alpha C_{max} + (1 - \alpha) C_{rand} \quad (1)$$

For each layer pair available in their three-month radar dataset, they calculated  $\alpha$  and plotted the average  $\alpha$  as a function of layer separation (any multiple of 360 m from 750 m above ground up to 10.5 km). The best fit was an exponential function and they denote the e-folding distance as  $Z_0$  and use this parameter as a measure of the overlap transition:

$$\alpha = \exp\left(-\frac{\Delta z}{z_0}\right) \quad (2)$$

For the three winter months at Chilbolton,  $Z_0$  was found to be 1.6 km.

We used the same period and data as HI00, except that the cloud mask was obtained from an algorithm similar to the active remote sensing cloud layer (ARSCL) (Clothiaux et al. 2000), but adapted specifically to the Chilbolton 94-GHz radar. The product used here is the QC reflectivity clutter flag that indicates if a pixel contains clear, cloud, clutter, mixture of cloud and clutter or no data. Figure 2 shows how the mean value of  $\alpha$  changes as a function of separation for contiguous cloud layers and non-contiguous cloud layers at Chilbolton. We found that  $Z_0$  was about 1.58 km for contiguous layers, in good agreement with HI00. We also agreed that for non-contiguous layers the overlap is random (Figure 2).

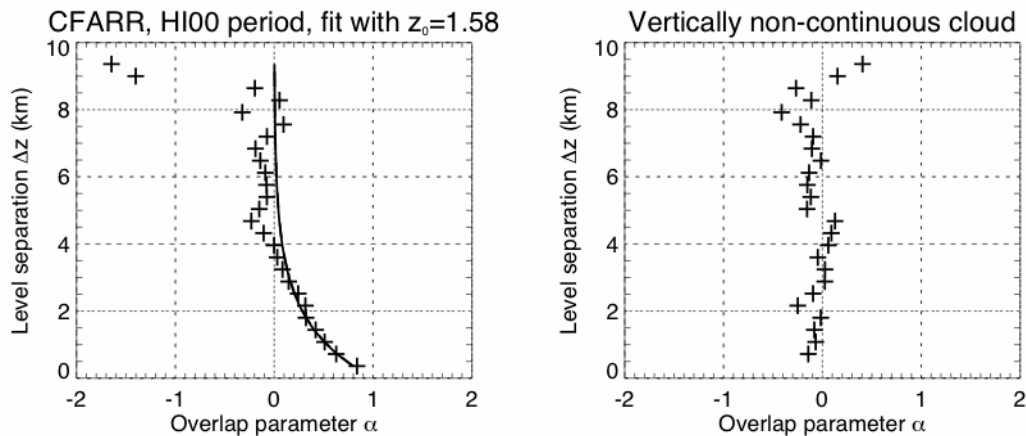


**Figure 2.** For contiguous cloud layers (left) and non-contiguous layers (right) at Chilbolton from November 1998 to January 1999, mean overlap parameter  $\alpha$  as a function of layer separation. A similar exponential behavior is found with the ARSCL cloud mask as in HI00 and the e-folding distances are very close. The solid line represents the exponential fit with  $Z_0=1.6$  km. Non-contiguous layers show an overlap very close to random.

## Comparison with Mace and Benson-Troth (2002)

We implemented the above technique to use on the ARSCL QC reflectivity clutter flag product at the SGP site and the Tropical Western Pacific (TWP) locale. Applying the same algorithm at the SGP site for the same period as in MBT02, we found  $Z_0$  close to 2 km, instead of 3.9 km in MBT02 (Figure 3). At TWP, MBT02 found  $Z_0=4.0$  km for Manus and 4.6 km for Nauru whereas we find  $Z_0=2.3$  and 1.8 km, respectively. To understand these differences and examine if the HI00 technique is strongly sensitive to how the radar cloud mask is obtained, we compared the ARSCL cloud mask against the cloud mask from MBT02 for July 1997 and January 1999 at the SGP site. The main differences we observed were as follows:

1. Both cloud masks filter out clutter near the surface (a real problem at the SGP site where insects can be detected as high as 4 km). However, their methods differ. This problem affects mainly warm months (April-October) so comparisons during winter should not be affected.

2. The cloud mask in MBT02 is derived using only one radar mode out of the four currently available, which are all used in ARSCL. One mode not used in MBT02 is the mode that is most sensitive to thin clouds (cirrus or shallow clouds); therefore, we expect more of these clouds to be taken into account when using ARSCL. Another consequence is that the MBT02 mask does not always detect cloud tops.
3. We noticed also that the MBT02 mask sometimes exhibited gaps in the reflectivity time series in precipitating clouds where this is not realistic. These empty profiles were found to cause an increase in  $Z_0$ . However, this seems to affect mostly summer statistics.

We found large differences between the  $Z_0$ s for July 1997, but the  $Z_0$ s were very close for January 1999 even if there were daily disparities. We are undergoing a thorough examination of the differences between the two cloud masks and their consequences for cloud overlap estimate. Consequently, for the time being, we decided to focus the rest of the study onto the cold months only (November-March) when we are certain that the technique used to extract the cloud fractions from the radar returns does not have a large impact on the overlap parameter.

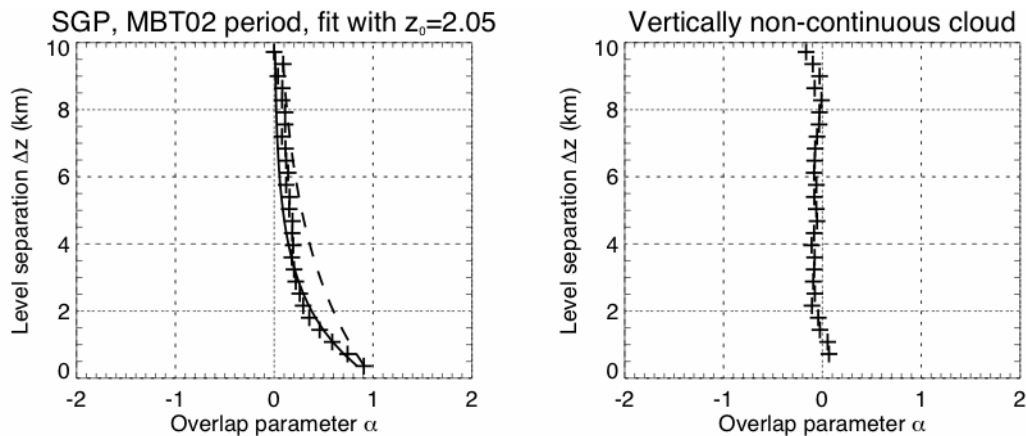


**Figure 3.** Same as Figure 2 but for the ARSCL radar cloud mask at the SGP site from March 1997 to December 2000. The dotted line shows the exponential fit with MBT02  $Z_0=3.9$  km, the dashed line shows the fit with  $Z_0=1.6$  km of HI00 and the solid line the fit with the estimated value of 2 km found with ARSCL.

## Impact of Dynamics at the SGP Site During the Winter Months

Information on the atmospheric dynamics was provided by the ARM reanalysis dataset RUC-2. We selected vertical velocity profiles provided in a  $10^\circ \times 10^\circ$  area centered on the SGP site of  $20 \times 20 \text{ km}^2$  pixel size. These files are available from 2002 onward, so we studied two winters worth of data (November 2002-March 2004). Figure 4 shows the distribution of  $\alpha$  as a function of separation. It can be noticed that the exponential fit does not take into account the large number of points where  $\alpha > 0.9$ . Therefore, there are two categories of situations: (1) situations where the overlap assumption for

contiguous layers should go from maximum to random over short distances, and (2) another group of situations where the overlap remains maximum over long distances as in the Geleyn and Hollingsworth (1979) model.

To understand how these features relate to atmospheric dynamics, we extracted for each pair of layers with an  $\alpha$  parameter the coincident 350, 500, and 850 mb vertical velocities from the RUC-2 files and for each of these pressure levels calculated the median vertical velocity per bin as defined for Figure 4. Figure 5 gives the distribution of 500 mb median vertical velocity as a function of separation and  $\alpha$ . This plot was obtained using both cold and warm months, but the cold months gave a similar plot, only noisier. The zone with the most negative values of  $\omega$  is much larger for 850 mb and much smaller for 350 mb but otherwise the general variations are similar. As expected, we notice that vertical velocities are larger for larger separation. However, Figure 5 also shows that the most vigorous upward velocities are also related to the larger values of  $\alpha$  at separations greater than 2 km. Undeniably, baroclinic and convective situations will tend to maintain a maximum overlap for most of the cloudy layer even in the limit of large separations. This was verified by isolating situations where precipitation was detected and comparing the distribution of  $\alpha$  with situations where precipitation was not detected. We found many more points at large separations where  $\alpha=1$  in the precipitating situations.

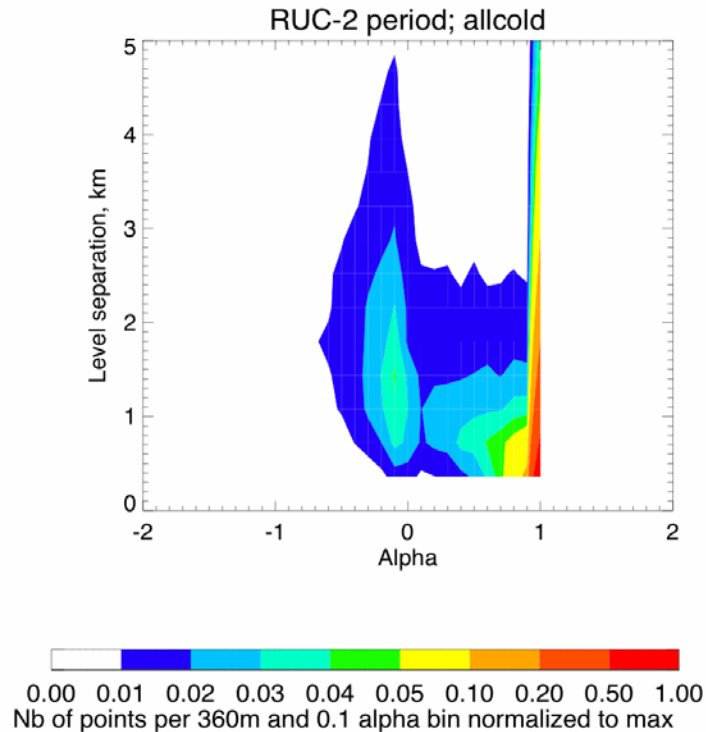


**Figure 4.** Normalized (to the maximum) number of points per 0.1  $\alpha$  bin and 360 m separation bin for all cold months during 2002-2004. For  $\alpha$  greater than 0.9 a significant number of points are found for large separations, which means that the exponential fit only partially describes the behavior of the overlap (for points with  $\alpha < 0.9$ ).

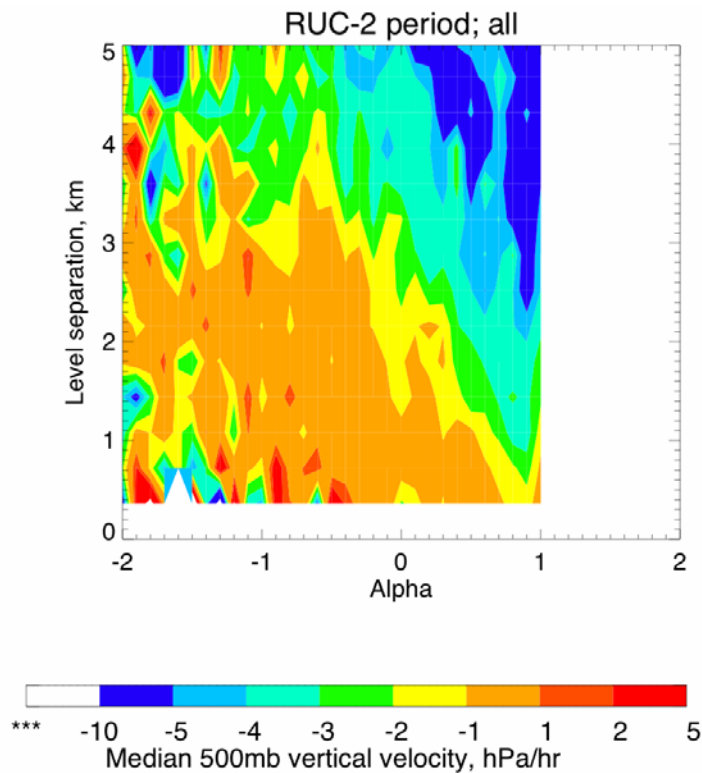


**Figure 5.** Median 500 mb vertical velocity as a function of  $\alpha$  and layer separation for all points found during 2002-2004. This includes the warm season but the plot for the cold season only shows the same general picture, only slightly noisier.

We isolated days during the cold season where a large number of points were found with  $\alpha=1$  and no precipitation was detected. Two types of situation emerged: one set of days were found with precipitation at some time not coincident with when  $\alpha$  was evaluated. These scenes showed some baroclinic or convective activity. The second set of scenes was more surprising. They all showed high clouds sedimenting as a function of time. Figure 6 shows an example of maximum overlap outside of a vigorous ascent type of situation. This scene occurred on 2004-01-12, and a significant number of points in the radar data were found with  $\alpha=1$ , in particular between 14:00 universal time coordinates (UTC) and 19:00 UTC. There was a TERRA overpass at 17:10 UTC and a MODIS true color image is shown as well. It reveals that the clouds are ridge-crest cirrus associated with a high pressure center southeast of the site as shown on the National Centers for Environmental Prediction/Department of Energy 500 mb height map. These cirrus clouds are sedimenting and in effect this type of precipitation also gives a maximum overlap.

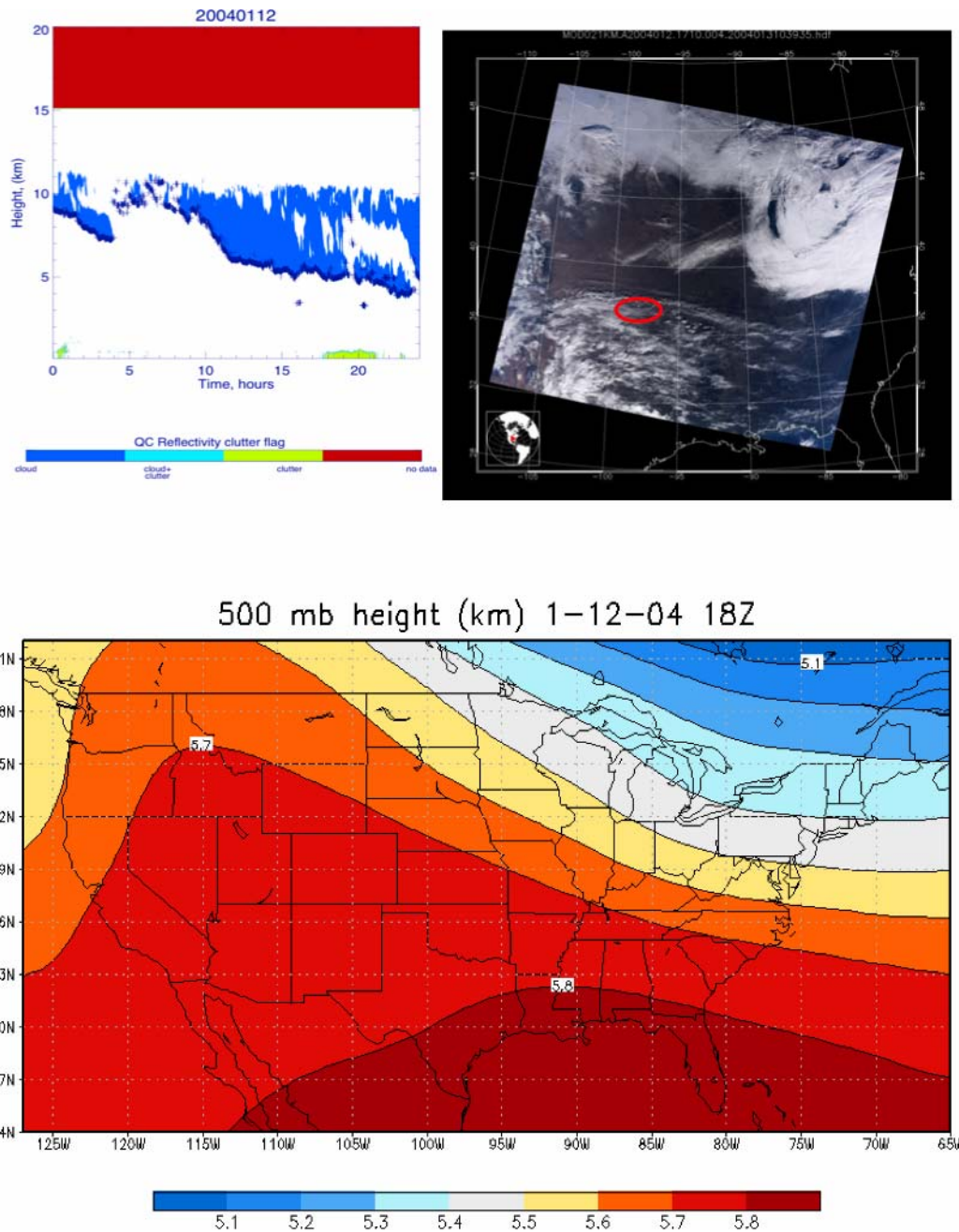


**Figure 6.** Radar cloud mask (top left) for 2004-01-12 where 39 layer pairs gave  $\alpha=1$  during periods 1-2, 9, 14-18 and 23 UTC; blue is cloudy, red is no data and green is clutter. The + signs show where the lidar detects cloud base. The top-right map shows the true color image measured with MODIS-TERRA at 17:10 UTC; the red circle is centered approximately on the SGP site. Ridge crest cirrus clouds can be seen above the site and the National Centers for Environmental Prediction 500 mb height map on the bottom confirms the presence of a high pressure center southeast of the SGP site.

## Overlap at Tropical Western Pacific

To verify that convective activity and associated precipitation have a tendency to force clouds into a maximum overlap for most of their vertical extent, we used radar ARSCL data for both TWP locations: C1 (Manus) and C2 (Nauru) instead of summer months at the SGP site. Figure 7 shows the normalized number of points for 0.1  $\alpha$  bins and 360-m separations at TWP-C1 (Manus) and for TWP-C2 (Nauru). The difference between the two figures indicates how TWP-C1 is dominated by deep convection where cloudy layers have large vertical extent and a large number of points with  $\alpha=1$  at large separations. TWP-C2 displays more suppressed conditions with shallower clouds but still a large number of points with  $\alpha=1$  at large separations. TWP-C1's  $Z_0$  was found to be greater than that at TWP-C2, which would be expected with more vigorous convection and clouds of larger vertical extent on average. However, in MBT02, the reverse was found, where clouds were maximally overlapping for longer separations at TWP-C2 than at TWP-C1. This needs to be investigated further.

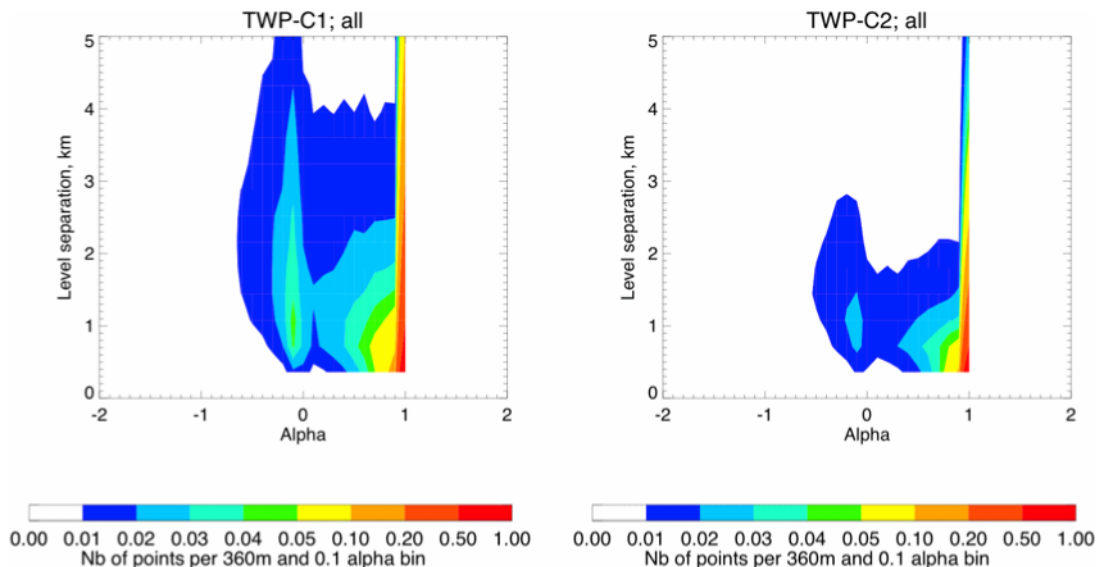


**Figure 7.** Normalized (to the maximum) number of points as a function of  $\alpha$  in 0.1 bins and 360 m separations at TWP-C1 (Manus; left) and TWP-C2 (Nauru; right).

## Conclusions

We found that indeed atmospheric dynamics has a large impact on how cloudy layers will overlap and we somewhat disagree with previous studies. Using the wintertime radar ARSCL cloud mask at SGP, we found that a significant number of clouds displayed a maximum overlap for large separations, while HI00 claimed that all clouds tend to rapidly overlap randomly as layer separations increase. Dynamics in baroclinic or convective situations where vertical velocities are ascending will preserve a maximum overlap of the cloudy layer to large separation. In addition, precipitation is associated with baroclinic

and convective regimes and displays a maximum overlap too over large separations. However, in addition, we also found situations with no ascending motion and no precipitation where clouds displayed maximum overlap at large separations. These situations showed slowly sedimenting high (ice) clouds. These clouds are more important than precipitation in the radiation budget so we need to take these into account too for the parameterisation of cloud overlap in models.

## Acknowledgements

This work was supported by an Interagency Agreement with the Atmospheric Radiation Measurement Program of the U.S. Department of Energy. The authors would like to express their gratitude to Sally Benson-Troth and Jay Mace as well Pavlos Kollias and Eugene Clothiaux for their time and effort to understand and explain to us the differences between ARSCL and MBT02.

## References

- Clothiaux EE, TP Ackermann, GC Mace, KP Moran, RT Marchand, MA Miller, and BE Martner. 2000. "Objective determination of cloud heights and radar reflectivities using a combination of active remote sensors at the ARM CART sites." *Journal of Applied Meteorology* 39:645-665.
- Geleyn, J-F, and A Hollingsworth. 1979. "An economical analytical method for the computation of the interaction between scattering and line absorption of radiation." Contributed *Journal of Atmospheric Physics* 52:1-16.
- Hogan, RJ, and AJ Illingworth. 2000. "Deriving cloud overlap statistics from radar." *Quarterly Journal of the Royal Meteorological Society* 126:2903-2909.
- Mace, GG, and S Benson-Troth. 2002. "Cloud-layer overlap characteristics derived from long-term cloud radar data." *Journal of Climate* 15:2505-2515.